

# Three-Dimensional Lightning Characteristics Relative to Reflectivity and Airflow Structure in Winter Thunderstorm

*Masahide Nishihashi\*<sup>1</sup>, Chusei Fujiwara<sup>2</sup>, Kenichi Kusunoki<sup>1</sup>, Satoru Yoshida<sup>1</sup>, Syugo Hayashi<sup>1</sup>, Hanako Inoue<sup>1</sup>, Ken-ichiro Arai<sup>1</sup>, Ken-ichi Shimose<sup>1</sup>, Ryohei Kato<sup>1</sup>, Sadao Saito<sup>1</sup>, Eiichi Sato<sup>1</sup>, Wataru Mashiko<sup>1</sup>, and Hiroto Suzuki<sup>2</sup>*

<sup>1</sup>Meteorological Research Institute, 1-1 Nagamine, Tsukuba, Ibaraki 305-0052, Japan; mnishiha@mri-jma.go.jp

<sup>2</sup>East Japan Railway Company, 2-479 Nisshin-cho, Kita-ku, Saitama 331-8513, Japan

## Abstract

A winter thunderstorm was observed in the Shonai area in the northern part of Japan on 30 November 2010. Data from three-dimensional lightning mapping system and two X-band Doppler radars were used to analyze the spatial-temporal relationship between winter lightning channel, reflectivity core, and airflow structure in the thunderclouds. A lightning leader propagating from a rim of echo region to the echo region with high reflectivity involving large vertical vorticity was visualized in 3D. This result indicates that strong updraft caused by airflow convergence in the precipitation system contributed to accumulate positive charges around -10°C level and enhance vertical vorticity by stretching on the convergence line.

## 1. Introduction

Many scientists have reported evidence that lightning activity is associated with severe weather such as wind gusts, tornadoes, and hail [1-5]. Recent studies reported that flash rate of total lightning (both intra-cloud (IC) and cloud-to-ground (CG) lightning) rapidly increases prior to the onset of severe weather events [4, 6-9], which Williams et al. [4] termed “lightning jumps.” Gatlin and Goodman [10] developed an algorithm to identify impending severe weather using the trends in the total flash rate. However, it is difficult to apply the same approach to winter lightning study because winter lightning in the coastal area of the Japan Sea exhibits various unusual characteristics that have not been observed in the summer in Japan or in any season in other geographical locations [11].

We have conducted field observations, which we have called “The Shonai Area Railroad Weather Project.” The Shonai area is located on the coast of the sea of Japan. The project was designed in 2007 to investigate the fine-scale structure of wind gusts using two X-band Doppler radars and a network of 26 surface weather stations in order to develop an automatic strong gust (vortex) detection system for railroads [12, 13]. We have focused on total lightning activity in winter to investigate the mechanism of the winter lightning discharge process and the application to the prediction of strong gusts.

Thus motivated, we developed a three-dimensional (3D) lightning mapping system for winter thunderstorms utilizing VHF broadband observation [14]. An observation network for winter lightning was constructed within comprehensive meteorological observation network in the Shonai area. This paper analyzes the spatial-temporal relationship between winter lightning channel, reflectivity core, and airflow structure (particularly vortex) in a cold-front thunderstorm on 30 November 2010.

## 2. Instruments and Methodology

### 2.1 3D Lightning Mapping System

We observed VHF broadband pulses radiated by leader progression using our 3D lightning mapping system in the Shonai area (Fig. 1). The VHF pulses were received with three discone antennas arranged in a triangle (20–30 m) and recorded on a high-speed digital oscilloscope (1.25-GHz sampling) with GPS digital timing data. The 2D mapping for azimuth and elevation of the VHF radiation sources was conducted by computing the arrival time differences of three pulses using a cross-correlation technique. Azimuth and elevation from two sites for a point source within a given time frame produce 3D lightning image using triangulation scheme.

### 2.2 X-band Doppler radars

We used radar reflectivity data and Doppler velocity data observed with two X-band Doppler radars located at the Shonai airport (MRI radar) and the Amarume station (JR-EAST radar) (Fig. 1). The JR-EAST radar has been operated in a plan position indicator (PPI) mode at one low-elevation angle ( $3.0^\circ$ ), while the number of elevation angles of the MRI radar was seven for volume scanning. Hence we estimated the wind field at 0.2 km in height inside thunderclouds conducting the dual-Doppler analysis. The spatial resolution of the grid point is 0.2 km.

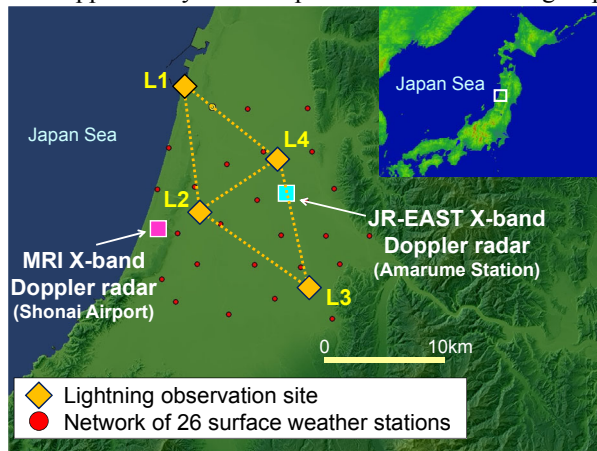


**Fig. 1.** Location of observation sites. The diamonds indicate the lightning observation sites. The squares denote the X-band Doppler radars and circles indicate the network of 26 surface weather stations.

### 3. Results

Figure 2 shows horizontal structure of a narrow cold-frontal rainband observed with the MRI radar at 1330:56 UTC on 30 November 2010. The rainband expanded linearly with a horizontal distance of about 22 km. The result of the dual-Doppler analysis shows that the obvious horizontal convergence ( $> 4 \times 10^{-3} \text{ s}^{-1}$ ) was formed in the reflectivity core (Fig. 2). Moreover the significant vertical vorticity area ( $2.5 \times 10^{-2} \text{ s}^{-1}$ ) is shown on the convergence line. Figure 2 also shows the horizontal distribution of the VHF radiation sources detected at 1332:15 UTC. The lightning leader progressed horizontally for 30 ms from the edge of the radar echo region to the reflectivity core through the echo-top height (10-25 dBZ, around 3 km in altitude) (indicated by red arrows in Figs. 2 and 3). This altitude is consistent with  $-10^\circ\text{C}$  level (2.9 km) retrieved from Meso-scale Analysis (MANAL) data released by the Japan Meteorological Agency. Figure 4 shows the spatial relationship in 3D between the reflectivity core and the VHF radiation sources. The VHF sources tend to be distributed around isosurface of 25 dBZ.

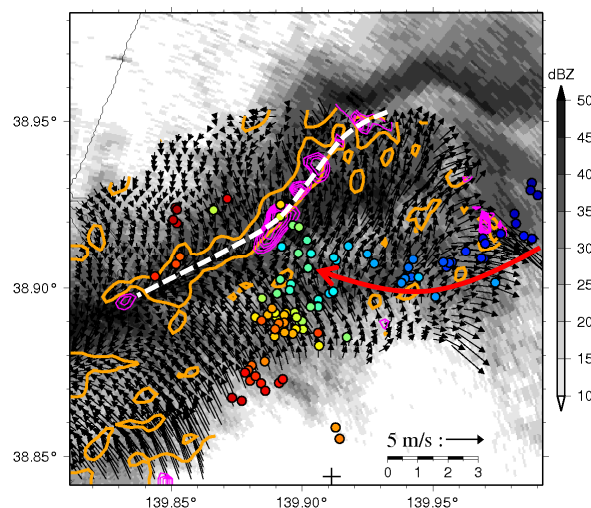


**Fig. 2.** Radar reflectivity and dual-Doppler synthesized storm-relative horizontal wind vectors at  $z = 0.2$  km at 1330:56 UTC. Orange contours show horizontal convergence ( $4 \times 10^{-3} \text{ s}^{-1}$ ). Dashed white line indicates estimated convergence line. Magenta contours denote vertical vorticity every  $0.2 \times 10^{-2} \text{ s}^{-1}$ , beginning at  $1 \times 10^{-2} \text{ s}^{-1}$ . Circles represent horizontal distribution of VHF radiation sources at 1332:15 UTC. Color of the VHF radiation sources indicates time increasing from blue through green to red.

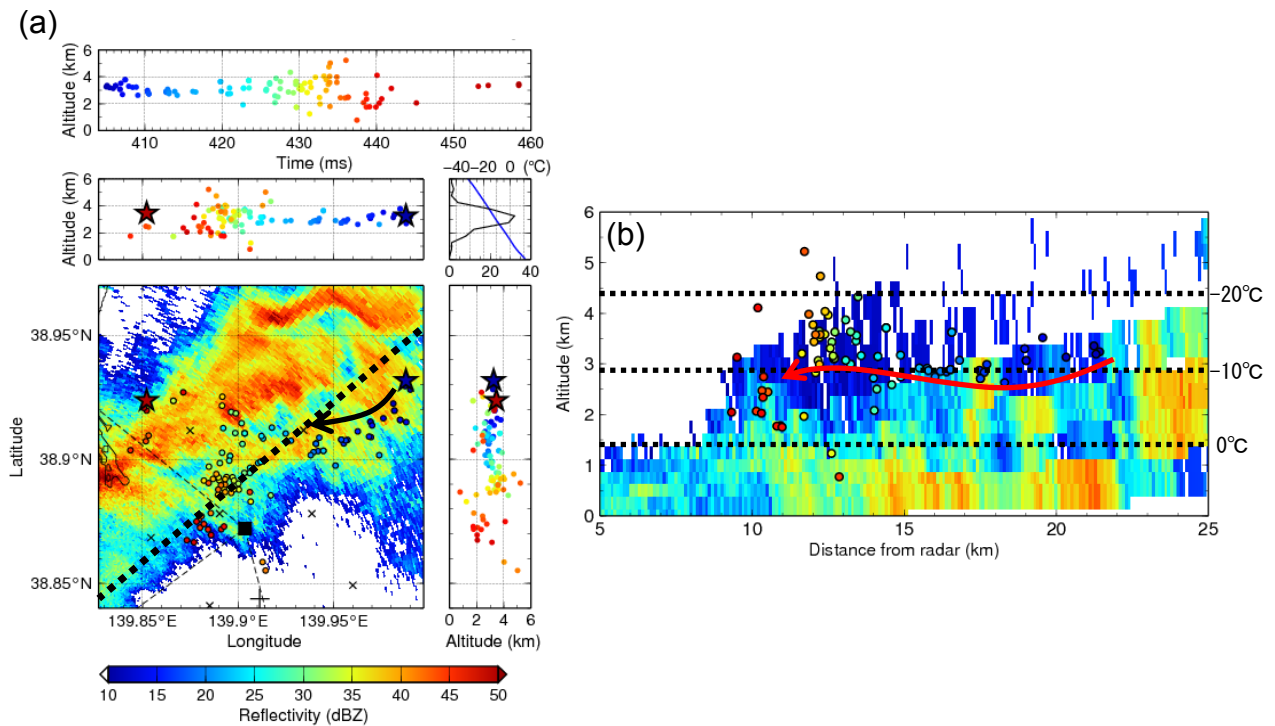


**Fig. 3. (a) 3D mapping of VHF radiation sources and radar reflectivity. Blue line indicates temperature profile retrieved from MANAL. (b) Vertical cross section of VHF radiation sources and radar reflectivity on the dashed line in (a).**

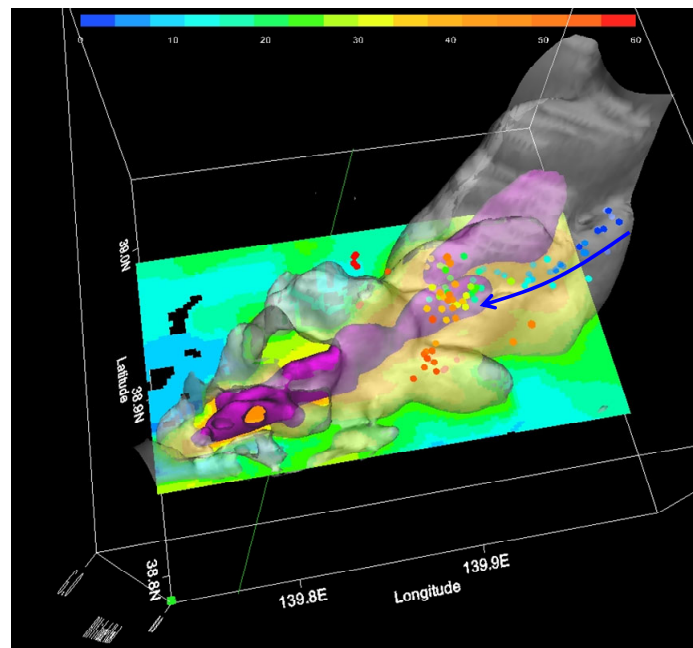


**Fig. 4. 3D presentation of 38-dBZ reflectivity isosurface (magenta), 25-dBZ reflectivity isosurface (gray), and VHF radiation sources (circles).**

#### 4. Discussion and Summary

This is a first result in winter thunderstorm on the coast of the Japan Sea that the lightning leader propagating from the rim of the echo region to the reflectivity core involving large vertical vorticity was visualized in 3D. Similar characteristics are shown in the subsequent flashes. We suggest that the strong updraft caused by airflow convergence

in the precipitation system led to the following two processes: (1) positive charge accumulation around  $-10^{\circ}\text{C}$  level associated with ice-crystals advection after the charge separation through collisions between graupel and ice crystals caused by the rimming electrification mechanism [15], (2) vertical vorticity enhancement by stretching on the convergence line. The result indicates there is a spatial-temporal relationship between lightning discharges and vortex evolutions in winter thunderstorms.

## 5. References

1. S. J. Goodman, D. E. Buechler, P. D. Wright, and W. D. Rust, "Lightning and precipitation history of a microburst - producing storm," *Geophys. Res. Lett.*, **15**, 1988, pp. 1185-1188.
2. D. R. MacGorman, D. W. Burgess, V. Mazur, W. D. Rust, W. L. Taylor, and B. C. Johnson, "Lightning Rates Relative to Tornadic Storm Evolution on 22 May 1981," *J. Atmos. Sci.*, **46**, 1989, pp. 221-251.
3. E. R. Williams, M. E. Weber, and R. E. Orville, "The Relationship Between Lightning Type and Convective State of Thunderclouds," *J. Geophys. Res.*, **94**, 1989, pp. 13213-13220.
4. E. Williams, B. Boldi, A. Matlin, M. Weber, S. Hodanish, D. Sharp, S. Goodman, R. Raghavan, and D. Buechler, "The behavior of total lightning activity in severe Florida thunderstorms," *Atmos. Res.*, **51**, 1999, pp. 245-265.
5. R. J. Kane, "Correlating Lightning to Severe Local Storms in the Northeastern United States," *Wea. Forecasting*, **6**, 1991, pp. 3-12.
6. S. J. Goodman, R. Blakeslee, H. Christian, W. Koshak, J. Bailey, J. Hall, E. McCaul, D. Buechler, C. Darden, J. Burks, T. Bradshaw, and P. Gatlin, "The North Alabama Lightning Mapping Array: Recent severe storm observations and future prospects," *Atmos. Res.*, **76**, 2005, pp. 423-437.
7. S. M. Steiger, R. E. Orville, and L. D. Carey, "Total Lightning Signatures of Thunderstorm Intensity over North Texas. Part I: Supercells," *Mon. Wea. Rev.*, **135**, 2007, pp. 3281-3302.
8. C. J. Schultz, W. A. Petersen, and L. D. Carey, "Preliminary Development and Evaluation of Lightning Jump Algorithms for the Real-Time Detection of Severe Weather," *J. Appl. Meteor. Climatol.*, **48**, 2009, pp. 2543-2563.
9. C. J. Schultz, W. A. Petersen, and L. D. Carey, "Lightning and Severe Weather: A Comparison between Total and Cloud-to-Ground Lightning Trends," *Wea. Forecasting*, **26**, 2011, pp. 744-755.
10. P. N. Gatlin, and S. J. Goodman, "A Total Lightning Trending Algorithm to Identify Severe Thunderstorms," *J. Atmos. Oceanic Technol.*, **27**, 2010, pp. 3-22.
11. V. A. Rakov, and M. A. Uman, *Lightning: Physics and Effects*, Cambridge Univ. Press, 2003, 687 pp.
12. K. Kusunoki, T. Imai, H. Suzuki, T. Takemi, K. Bessho, M. Nakazato, W. Mashiko, S. Hayashi, H. Inoue, T. Fukuhara, T. Shibata, and W. Kato, "An overview of the Shonai area railroad weather project and early outcomes," Fifth Eur. Conf. on Radar in Meteor. and Hydrol., Helsinki, Finland, 2008, P12.1.
13. H. Y. Inoue, K. Kusunoki, W. Kato, H. Suzuki, T. Imai, T. Takemi, K. Bessho, M. Nakazato, S. Hoshino, W. Mashiko, S. Hayashi, T. Fukuhara, T. Shibata, H. Yamauchi, and O. Suzuki, "Finescale Doppler Radar Observation of a Tornado and Low-Level Mesocyclones within a Winter Storm in the Japan Sea Coastal Region," *Mon. Wea. Rev.*, **139**, 2011, pp. 351-369.
14. M. Nishihashi, K. Shimose, K. Kusunoki, S. Hayashi, K. Arai, H. Y. Inoue, W. Mashiko, M. Kusume, and H. Morishima, "Three-Dimensional VHF Lightning Mapping System for Winter Thunderstorms," *J. Atmos. Oceanic Technol.*, **30**, 2013, pp. 325-335.
15. T. Takahashi, "Thunderstorm Electrification—A Numerical Study," *J. Atmos. Sci.*, **41**, 1984, pp. 2541-2558.